Fabrication of high content carbon nanotube-polyurethane sheets with tailorable properties

Rubi, Yadienka Martinez; Ashrafi, Behnam; Jakubinek, Michael B.; Zou, Shan; Laqua, Kurtis; Barnes, Michael; Simard, Benoit

Publisher's version / Version de l'éditeur:
https://doi.org/10.1021/acsami.7b09208
ACS Applied Materials and Interfaces, 2017-08-22

Fabrication of High Content Carbon Nanotube-Polyurethane Sheets with Tailorable Properties

Yadienka Martinez-Rubi, [†] * *Behnam Ashrafi,* [‡] *Michael B. Jakubinek,* [†] *Shan Zou,* [§] *Kurtis Laqua,* [‡] *Michael Barnes,* [†] *Benoit Simard*[†]*

[†] Security and Disruptive Technologies, National Research Council Canada, Ottawa, ON, Canada

[‡] Aerospace, National Research Council Canada, Montreal, QC, Canada

[§]Measurement Science and Standards, National Research Council Canada, Ottawa, ON, Canada

ABSTRACT: We have fabricated carbon nanotube (CNT)-polyurethane (TPU) sheets via a one-step filtration method that uses a TPU solvent/non-solvent combination. This solution method allows for control of the composition and processing conditions, significantly reducing both the filtration time and the need for large volumes of solvent to debundle the CNTs. Through an appropriate selection of the solvents and tuning the solvent/non-solvent ratio, it is possible to enhance the interaction between the CNTs and the polymer chains in solution and improve the CNT exfoliation in the nanocomposites. The composition of the nanocomposites, which defines the characteristics of the material and its mechanical properties, can be precisely controlled. The highest improvements in tensile properties were achieved at a CNT:TPU weight ratio around

35:65 with a Young's modulus of 1270 MPa, stress at 50 % strain of 35 MPa, and strength of 41 MPa, corresponding to ~10 fold improvement in modulus and ~7 fold improvement in stress at 50 % strain, while maintaining a high failure strain. At the same composition, CNTs with higher aspect ratio produce nanocomposites with greater improvements (e.g. strength of 99 MPa). Electrical conductivity also shows a maximum near the same composition, where it can exceed the values achieved for the pristine nanotube buckypaper. The trend in mechanical and electrical properties was understood in terms of the CNT-TPU interfacial interactions and morphological changes occurring in the nanocomposite sheets as a function of increasing the TPU content. The availability of such a simple method and the understanding of the structure-properties relationship are expected to be broadly applicable in the nanocomposites field.

Keywords: Carbon nanotubes, polymer composites, morphology, mechanical properties, conductivity, AFM

INTRODUCTION

The incorporation of CNTs into polymer matrices has been extensively studied, demonstrating the potential of CNTs for improving the mechanical, thermal and electrical properties of polymer composites[1,2] and expanding the applications of polymer materials. Nanocomposites are most commonly fabricated by dispersing CNTs into a polymer matrix via solution or melt processing.[3] Interfacial interactions between CNTs and the matrix, as well as the CNT dispersion and distribution are paramount to transfer the exceptional properties of CNTs to polymer composites. The development of high nanotube content composites is also of interest in the nanocomposite

field; however, the incorporation of a high content of well-dispersed nanotubes into polymer composites can be impractical due to re-agglomeration of the nano-filler and a significant increase in viscosity. Fabrication of high nanotube content composites is usually carried out by solution casting[4] or resin-infiltration of CNT sheets (buckypaper).[4-6] This approach has yielded some of the highest mechanical performances for CNT composites. However the CNT sheets that have led to the best mechanical properties,[7,8] such as those produced from long CNTs collected directly during synthesis, are not yet broadly available in large quantities. Additionally, uniform polymer infiltration can be challenging due to long periods of time (12- 24 hours[4]) that can be necessary to fully infiltrate a preformed buckypaper. It is still challenging to attain a simple and economical method that improves CNT individualization, CNT distribution and CNT-polymer interfacial interactions to enable the production and exploitation of nanocomposite products.

Here we report a one-step filtration process for the direct fabrication of high-content CNT-thermoplastic polyurethane (TPU) composite sheets that could also be applied to different polymer matrices. TPU are block copolymers of the $(AB)_n$ type. They consist of nanophase separated hard segments (HS) and soft segments (SS) and can be tailored according to the desired application requirements. Ductile elastomeric polyurethanes, which are characterized by low stiffness and low stress at low strain but high ductility and toughness, are considered a promising matrix in balancing the mechanical properties of CNT reinforced polymers for the production of stiff, stronger, yet tough thermoplastic polymer composites.[9-11] We show the fabrication of non-woven CNT-TPU composite sheets of variable composition using the one-step filtration process, along with analysis of the morphological and compositional control based on adsorption of TPU on the surface of CNTs. The CNT-TPU sheets have tailored properties

showing significant enhancement in tensile properties and electrical conductivity. Tensile properties and electrical conductivity show an optimum near the same composition. We also employ atomic force microscopy (AFM) to map the elastic modulus at the nano-to-micro scale for comparison to the bulk tensile properties. Due to their straightforward production and handling, high nanotube content, and superior properties in comparison to dispersed CNT composites, the resulting conductive, lightweight sheets are of interest for various applications including improved damage tolerance and electrical properties of laminate composites, self-sensing and electromagnetic shielding.

MATERIALS AND METHOS

NC7000TM industrial grade MWCNTs (CNTs) were obtained from Nanocyl SA (Belgium). These MWCNTs have average diameter (d) of 9.5 nm, average length (L) of 1.5 μm, density (ρ_{CNT}) of 1.7 g/cm^3, and BET surface area of 250-300 m^2/g according to the manufacturer specifications. Longer nanotubes, XL-MWCNTs (XL-CNTs) of L = 1-3 mm, d = 20-40 nm and ρ_{CNT} = 2.1 g/cm^3 were obtained from NanoTechLabs (Yadkinville, NC). Composites of XL-CNTs were compared to the more common micron-length scale CNTs. The polyurethane was a thermoplastic ester based polyurethane (UAF 472 by Adhesive Films Inc., Pine Brook, NJ) of density 1.19 g/cm^3 and a shore hardness A of 85.

The CNT-TPU nanocomposite sheets were fabricated by a one-step filtration method using a suspension of CNT dispersed in a TPU solvent/non-solvent mixture.

Acetone/methanol: TPU dissolved in acetone was combined with a suspension of CNTs in a polymer non-solvent (methanol). For 3.5 cm diameter samples, 30 mg of CNTs where suspended in 80 mL of methanol using a sonication bath (Fisher Scientific FS110) for 1hour followed by horn sonication (Branson Sonifier 250, 30% output, 50% duty cycle) for 5 min and bath sonication for 15 min. The CNT suspension was then added to the TPU solution containing the required amount of TPU (Table 1) dissolved in 75 mL of acetone and mixed with bath sonication for 1 hour followed by horn sonication for 5 min and bath sonication for 1hour.

DMF/methanol: 30 mg of CNTs were dispersed in 90 mL of DMF. TPU dissolved in 10 mL of DMF was combined with the CNTs and then combined with 150 mL of methanol using bath and horn sonication as described above.

The mixtures were filtered, using a Venturi air pump, through a PTFE membrane (1.2μm pore size). Filtration was completed in 5-15 min. The wet nanocomposite sheets were immediately sandwiched between parchment and filter papers and dried flat at room temperature overnight, after which they were peeled from the filter membrane, placed between Teflon films and further dried at 75 °C in vacuum for 10 hours to remove residual solvent. The weight fraction of TPU in the final composites was determined by weighing the dried nanocomposites. For sorption evaluation, the amount of TPU adsorbed per unit mass of CNTs (C_{ads}) and its remaining concentrations in the solutions (C_{eq}) at equilibrium were determined as follow:

$$C_{ads} = \frac{m_{TPU,comp}}{m_{CNT}} = \frac{m_{comp} - m_{CNT}}{m_{CNT}}$$

$$C_{eq} = \frac{m_{TPU,sol}}{V_{sol}} = \frac{m_{i,TPU} - m_{TPU,comp}}{V_{sol}}$$

Where m_{CNT} and $m_{i,TPU}$ are the initial amounts of CNTs and TPU, respectively, and m_{comp} corresponds to the weight of the dried nanocomposite. $m_{TPU,comp}$, $m_{TPU,sol}$ and V_{sol} correspond to the amount of TPU adsorbed by the CNTs, the amount of TPU remaining in solution, and the volume (155 mL) of the solution, respectively.

Pristine buckypaper with CNTs from Nanocyl was obtained by vacuum filtration of the CNT suspension in methanol. For XL-CNTs it was necessary to use an aqueous solution with sodium cholate (1% by weight) to disperse the XL-CNTs prior to vacuum filtration as the longer CNTs were not sufficiently dispersed in methanol alone.

Characterization:

Composition: The external volume of the samples was evaluated by cutting squares of 30 mm x 30 mm from the CNT-TPU composites. The thickness was measured with a Marathon Digital Electronic Micrometer having a resolution of 0.001mm. The volume fraction of nanotubes ($V_{f,CNT}$), TPU ($V_{f,TPU}$) and pores/voids ($V_{f,voids}$) in the samples were estimated using equations 1, 2 and 3:

$$V_{f,CNT} = \frac{\rho_{Comp}}{\rho_{CNT}} W_{f,CNT} \qquad (1)$$

$$V_{f,TPU} = \frac{\rho_{Comp}}{\rho_{TPU}} W_{f,TPU} \qquad (2)$$

$$V_{f,voids} = 1 - V_{f,TPU} - V_{f,CNT} \qquad (3)$$

Where ρ_{Comp}, ρ_{CNT} and ρ_{TPU}, are the nanocomposite sheet, CNT and TPU densities, respectively. ρ_{Comp} was obtained by dividing the mass of the CNT-TPU composite sheets by their

external volume, while the manufacturer value was used for ρ_{CNT}. $W_{f,CNT}$ and $W_{f,TPU}$ correspond to the weight fraction of CNT and TPU, respectively in the CNT-TPU composite sheets.

Imaging and properties: Scanning electron microscopy (SEM) images were taken with a Hitachi High Technologies S-4800v. Tensile testing was performed using a micro-tensile test frame (Fullam Substage Test Frame). A minimum of five strips (~30 mm x 2mm) of each material were tested at a displacement rate of 5 mm/min and initial gauge length of ~20 mm. Electrical conductivity ($\sigma = 1/R_s t$) was calculated from measurements of sheet resistance (R_s) and average thickness (t). The sheet resistance was measured using the van der Pauw method,[12] where 4 contacts points were made directly with tungsten probes of a probe station (Cascade Microtech) to the perimeter of the sample in a counter-clockwise order. Two independent Keithley 2400 source-measure units were used to source current and measure voltages. Current reversal and reciprocal measurements, rotating the current source and voltmeter though all four contact pairs, were employed to improve the measurement accuracy. The measurement was repeated using multiple current levels to ensure consistency of the results, independent of measurement current.

Atomic force microscopy (AFM) imaging and elastic modulus mapping: AFM measurements were carried out using the MultiMode AFM with the NanoScope V controller (Bruker Nano Surfaces Division, Santa Barbara, CA, USA), in Peak Force QNM mode. The peak force with which the tip taps the sample surface was always kept at the lowest stable imaging level of 200 – 400 pN. Silicon nitride ScanAsyst-Air AFM probes (Bruker AFM Probes, Camarillo, CA, USA) were used in all peak force feedback measurements. Their manufacturer specified typical tip diameter and spring constants are 2 nm and 0.4 N/m, respectively. While images of sizes of up to 20 μm x 20 μm were acquired to ensure good homogeneity nanotube networks, all the images

used to measure modulus were 500 nm x 500 nm in size, acquired with the 512 x 512 pixel resolution, and the AFM probe cantilever was vertically oscillated at 2 kHz, at a lateral scan rate of 1 Hz. In this way the lateral pixel size is approximately 1 x 1 nm^2. The elastic modulus values were analyzed in terms of the distribution of Derjagin-Muller-Toropov (DMT) moduli over the investigated area. In order to obtain reliable results of mechanical properties through AFM, the "relative calibration method" was adopted; details about the "relative method" can be found in the instrument manual provided by Gojzewski et al.[13] Two reference samples were selected for calibration: polystyrene and polydimethylsiloxane gel with elastic modulus of 2.7 GPa and 3.5 MPa, respectively. The calibration was always carried out before any measurements of the samples characterized.

RESULTS AND DISCUSSIONS

Solubility modulation is a simple method that has been used to control the morphology of various materials.[14,15] The use of a non-solvent (e.g. methanol) can induce phase separation of the UAF 472 TPU dissolved in a good solvent (e.g. acetone, THF or DMF) starting at a specific solvent/non-solvent volume ratio. In the absence of CNTs, a cloudy suspension is obtained (Figure 1a) when methanol is added to a solution of TPU in acetone to a 50:50 vol.% solvent ratio due to phase separation. Figure 1b shows a schematic representation of the process used for the fabrication of the CNT-TPU composite sheets using the solvent/non-solvent approach. It was evident that when CNTs were present, at the compositions studied, no free polymer particles were visible in the solvent mixture (Figure 1b). In the presence of CNTs, upon mixing with the

non-solvent, the polymer separates from the solution and immobilizes onto the surface of the CNTs as result of non-covalent van der Waals interactions between CNTs and TPU. The large surface area of CNTs (~250 m^2/g) offers abundant sites for the precipitation of the polymer. The obtained CNT-TPU suspension can be readily vacuum-filtered in about 5-15 min, depending on the composition, and a smooth homogeneous sheet is easily peeled from the filter membrane after drying at room temperature (Figure 1c and 1d). It was observed that when only a good solvent for TPU (e.g. acetone or THF) is used instead of the solvent/non-solvent combination, increasing the amount of TPU in solution only leads to significantly longer filtration times (30 min to 5h) and the TPU content in the final composite sheets increases only slightly despite significantly increasing the TPU/CNT ratio in the solution mixture (Table S1). Conversely, at the constant methanol/acetone volume ratio (~50:50 vol%) the TPU content in the nanocomposites can be precisely controlled by simply varying the concentration of TPU in the acetone solution.

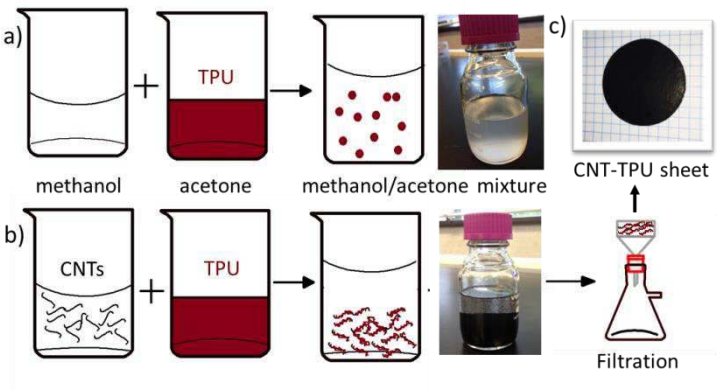

Figure 1. Schematics of the one-step CNT-TPU sheets fabrication method. a) TPU phase separation in the solvent/non-solvent mixture. b) TPU immobilization on the CNTs surface. c) Photo of a TPU-CNT composite sheet.

Table 1 summarizes the compositional properties of nanocomposite sheets with different CNT/TPU weight ratios obtained by this procedure. The amount of TPU in the final composite sheet is determined by the TPU partition coefficient between the liquid (acetone/methanol mixture) and the solid phase (CNT surface) and, for the relevant compositions studied here, it was found to be close to 70 % of the initial amount of TPU dissolved in acetone (see section 3.2 below). Using this procedure, high CNT content nanocomposite sheets with different CNT:TPU weight ratios were obtained with increasing density as the TPU content increased (Table 1). Similar materials can also be obtained by infiltration of a preformed buckypaper by changing the concentration and/or volume of the TPU solution used for the infiltration. However, this methodology requires first the fabrication of the buckypaper, which can be a fragile material (difficult to handle), and then proceeding with the infiltration step.[4,9] The buckypaper infiltration approach offers less control of the composition and CNT dispersion than the solvent/non-solvent approach. Additionally, long infiltration times are required to achieve full buckypaper impregnation. Hence the present approach offers several advantages and can be more convenient for fabrication of larger samples.

Table 1. Properties of the CNT-TPU sheets prepared from the acetone/methanol mixture. Note that in the sample labels (CNPU-xx), xx indicates the percentage of TPU by weight in the composite.

	In solution	**CNT-TPU Sheets**					
Sample	CNT/TPU wt. ratio	CNT-TPU wt. ratio	Density (g/cm^3)	Thickness (μm)	Volume fraction (vol.%)		
					CNT	TPU	Void
MWCNT	1:0	100:0	0.27	120	16	0	84

CNPU-45	1:1	55:45	0.57	100	18	21	60
CNPU-55	1:1.5	45:55	0.70	98	19	31	50
CNPU-65	1:2.5	35:65	0.94	97	19	51	29
CNPU-70	1:3.5	30:70	0.98	119	16	60	24
CNPU-80	1.5	20:80	1.12	139	13	75	12
CNPU-90	1:10	10:90	1.07	271	7	80	13
TPU	0:1	0:100	1.19	-	0	100	0

*Micron-length CNTs from Nanocyl

The measured density of the CNT-TPU sheets indicates that the nanocomposites are porous in nature even at relatively high TPU weight fractions. Interestingly CNPU-65 has the smallest thickness despite starting with an equivalent mass of CNTs for all samples. The volume fraction of the nanocomposite components were calculated using equations 1-3 and results are shown in Table 1. With increasing amount of TPU in solution, the volume fraction of TPU in the sheets increases, as expected, and the free volume (voids) decreases. However, the CNT volume fraction remains almost constant (18-19 vol.%), and higher than for the MWCNT-only buckypaper comparison, for up to ~50 vol.% TPU (CNPU-65). At higher TPU content (e.g., CNPU-70) the volume fraction of CNTs decreases as the TPU content increases.

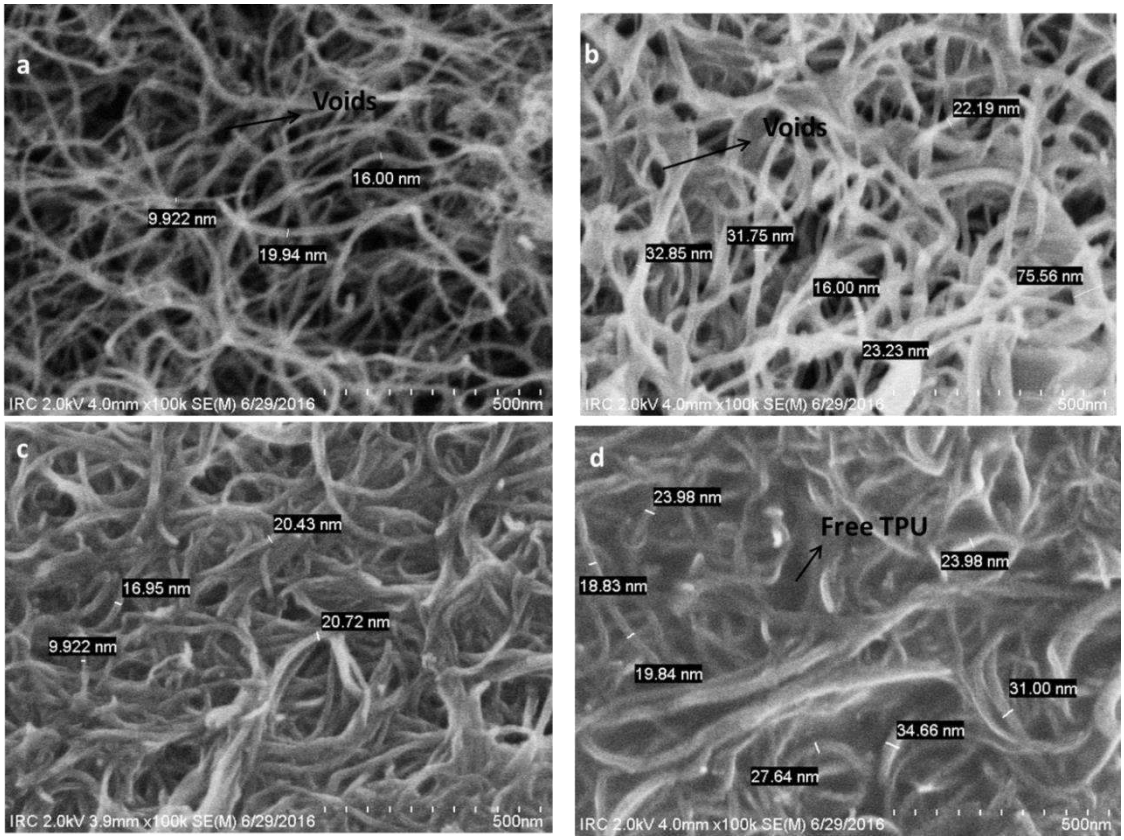

Figure 2. SEM images of the surface of (a) pristine CNT buckypaper and (b) CNPU-55 (c) CNPU-65 (d) CNPU-80 composite sheets.

Figure 2 shows typical SEM images of the surface of a pristine CNT buckypaper, obtained by filtration of CNTs dispersed in methanol, together with nanocomposite sheets at different TPU contents (additional images in Figure S1). The morphology of the nanocomposite sheets resembles that of composites made by buckypaper polymer infiltration.[9] In the pristine buckypaper, individual CNTs (~10 nm) are observed as well as ~15 to 20 nm bundles forming a low density network with high void content. The nanocomposites also show a nanofiber-like

morphology but with larger diameters (~ 20 to 30 nm) than in the pristine buckypaper, which suggests the presence of TPU coating the surface of individual CNTs and CNT bundles.

The diameters of the CNT-TPU "fibers" are very similar in nanocomposite samples CNPU-55 and CNPU-65, but appear slightly larger for sample CNPU-80 with a higher TPU content. The trend in the bulk density is consistent with SEM images showing the amount of voids decreases with increasing TPU content. Sample CNPU-80 shows the fiber-like morphology apparently embedded with free TPU (Figure 2d) and consequently a significant reduction in visible voids (higher density). The morphological analysis indicates that, through solubility modulation, the TPU polymer chains form a stable shell around the CNTs and suggests that different degrees of exfoliation might be achieved in solution when increasing the TPU/CNT ratio. This better exfoliation could lead to a more dense structure, which is also apparent from the lower thickness measured for the CNPU-65 sample (Table 1). Similar network compaction has been reported by others during buckypaper modification with polypyrole. In that case the authors suggested that the conjugated polymer wrapping might be binding the network together more tightly with a more efficient packing,[16] which also appears to be the case with CNT-TPU sheets in the present investigation. Above a certain TPU/CNT ratio, between the composition of CNPU-65 and CNPU-80, further addition of TPU does not lead to additional CNTs debundling, CNT network densification or significant growth in the thickness of the TPU coating. After that point, excess free polymer simply coexists with TPU/CNT fibers. The free polymer in the structure is probably intercalated in the structure and it is responsible for the increase in the sheet thickness, which translates into a lower CNT volume fraction at the highest TPU contents evaluated (e.g. CNPU-70 and CNPU-80 in Table 1).

Adsorption Equilibrium Studies

Adsorption equilibrium studies are often performed to investigate the properties of adsorbents. For a two-component system of a sorbent (e.g. CNTs) and solution, a graph of the solute (e.g. TPU) concentration in the solid phase C_{ads} (mg/g) can be plotted as a function of the solute concentration in the liquid phase C_{eq} (mg/L) at equilibrium.[17] At equilibrium there is a defined distribution of the solute between the liquid and the solid phase, which can generally be expressed by one or more isotherms. Adsorption of contaminants onto CNTs has previously been studied for water decontamination; [18,19] however, to the best of our knowledge, adsorption isotherms have not been applied to describe surface modification of CNTs in the production of CNT-polymer composites.

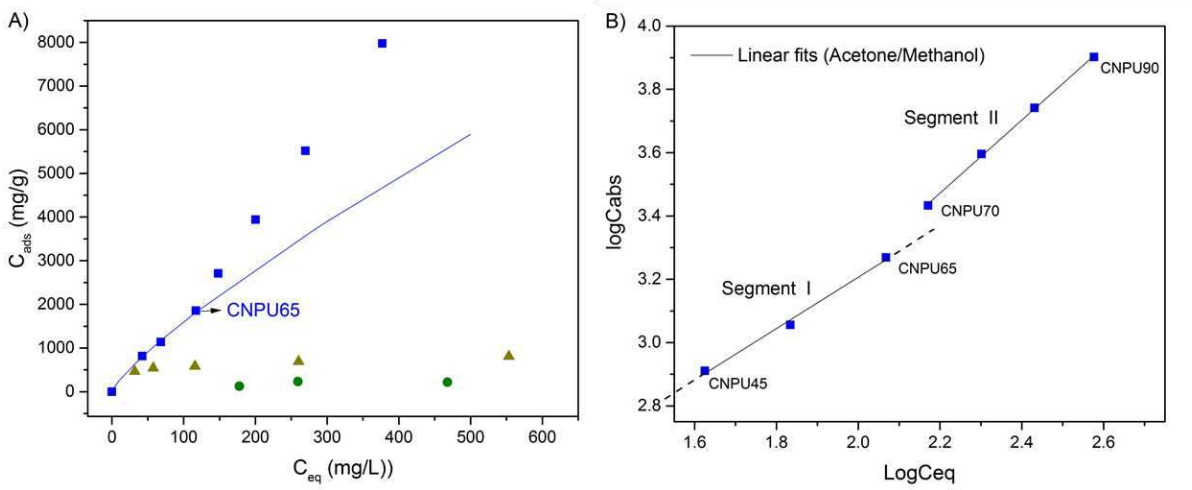

Figure 3. A) Adsorption data of TPU on CNTs in the acetone/methanol mixture (■), in acetone alone (▲) and in THF alone (●). (B) Linearized forms of the Freundlich isotherm for the adsorption shown in Figure 3A. The continuous blue line (Figure 3A) corresponds to the Freundlich isotherm (segment I only) in the acetone/methanol mixture.

Figure 3A shows the room temperature adsorption data of TPU on CNTs processed in the acetone/methanol mixture, as well as in acetone or THF alone. The use of a solvent/non-solvent mixture clearly increased the adsorption uptake of TPU by the CNTs as compared to samples prepared in a good solvent only. Moreover, for the same initial concentration of TPU, the higher the adsorption capacity the lower the concentration of TPU at equilibrium (C_{eq}), as determined by the partition coefficient. From these results we can conclude that, because of the CNT-TPU fiber-like morphology and relatively low C_{eq} of TPU (Figure 3A) in the solvent/non-solvent mixture, the CNT-TPU nanocomposites can be recovered by filtration in a very short time as a nonwoven sheet made of highly entangled and randomly oriented CNT-TPU fibers. In acetone and THF alone, the adsorption of TPU by the CNTs is quickly saturated, which limits the content of TPU in the nanocomposite sheets to low values while a high concentration of TPU in the solution significantly increases the filtration time. (e.g. weight ratio of ~ 80:20 in TFH with 3 h filtration time, Table S1). The conformation of the TPU chains on the CNT-TPU fibers likely also plays a role in the interaction with the solvent (solvent polarity and hydrogen bonding), which will also influence the filtration time and the packing of the structure.

The equilibrium experimental data for adsorbed TPU on CNTs in the acetone/methanol mixture were subjected to analysis based on Freundlich adsorption isotherm, which is purely empirical and it best describes adsorption on heterogeneous surfaces.[18,20] The following linearized Freundlich equation was used:

$$\log C_{abs} = \log K_F + 1/n \log C_{eq}$$

where C_{ads} is the amount of TPU adsorbed (mg/g), C_{eq} is the equilibrium concentration of TPU in solution (mg/L), K_F is the Freundlich constant (L/g), and 1/n is the Freundlich exponent. The linear plots of Freundlich isotherm for the adsorption of TPU on the CNTs (acetone/methanol mixture) is presented in Figure 3B. From the linearized form it is evident that if the data is separated in two segments (I and II), both segments are better described separately by this model. Linear fits return correlation coefficients of 0.988 for the data corresponding to compositions between CNPU-45 to CNPU65 (segment I) and 0.999 for compositions between CNPU-70 to CNPU-90 (segment II). The isotherm parameters K_F and 1/n , which are rough measures of the adsorption capacity and adsorption intensity of the adsorbent, were determined by the least-squares fitting to be 38 L/g and 0.8 respectively for segment I. Figure 3A (continuous blue line) shows the calculated isotherm using the Freundich parameters for the first segment. The K_F and 1/n parameters for segment II were found to be 9 L/g and 1.2 L/g, respectively. A value of 1/n = 1 signifies that the relative adsorption (adsorption partition) of the chemical was the same across the whole range tested, which is unusual (especially across the concentration range of two orders of magnitude often used). More normally, 1/n values will range from 0.1 to 1.0.[20;21] These values show that when the concentration of chemical under investigation increases, the relative adsorption decreases. This is indicative of saturation of adsorption sites available to the chemical, resulting in relatively less adsorption. The concentration range of segment I (CNPU-45 to CNPU-65) follows this behavior and is well-described by the Freundlich isotherm. However, if the concentration of TPU in the solvent/non-solvent mixture increases above the point of saturation a deviation from the predicted behavior occurs. Likely explanations are that additional TPU adsorbed by formation of a thicker coating and/or it is deposited by phase separation between CNT-TPU fibers (cooperative adsorption). These results are in agreement with the

morphological characterization by SEM (Figure 2), and with the properties of the nanocomposite sheets (Table 1). Up to sample CNPU-65 the incremental addition of TPU might be increasing CNT exfoliation (increasing surface area) and increasing CNT coverage with TPU, while the CNT vol.% and CNT-TPU sheet thickness remain almost constant. Above the saturation concentration, additional TPU is instead deposited by phase separation, which increases the nanocomposite sheet thickness and the CNT vol.% decreases.

Mechanical and electrical properties of the nanocomposite sheets

Figure 4a shows typical tensile stress-strain curves of the CNT-TPU nanocomposite sheets fabricated from the acetone/methanol mixture. Results for neat TPU are also shown for comparison. Table 2, Figures 4b and 4c summarize the mechanical properties as a function of TPU content (CNT/TPU weight ratio). The polyurethane used in this study is a thermoplastic rubber with manufacturer reported values of 34 MPa, 4 MPa and 8 MPa for the tensile strength, stress at 100% strain ($\sigma_{\varepsilon=100\%}$) and stress at 300 % strain ($\sigma_{\varepsilon=300\%}$), respectively. The tensile tests show that the tensile strength (σ_{fail}) and Young's modulus (E) initially increase as the TPU wt.% increases in the composite films, with maximum values at the CNPU-65 composition, and then decrease with increasing TPU. These results correlate with observations from morphological and compositional properties of the nanocomposites described above and support the hypothesis that, at this composition (CNPU-65), better CNT exfoliation and optimal CNT surface coverage is achieved, which in turn leads to an optimal packing of CNT-TPU fibers. Further addition of TPU leads to a lower reinforcement effect, which can be explained as a result of additional TPU not

only decreasing the void vol.% in the obtained CNT-TPU sheets but also depositing between CNT-TPU fibers and producing nanocomposites sheets with a lower CNT vol.%.

At the "optimal" composition, E of 1.27 GPa, $\sigma_{\varepsilon=50\%}$ of 35 MPa, and σ_{fail} of 41 MPa are obtained corresponding to ~10 fold improvement in E, ~7 fold improvement in $\sigma_{\varepsilon=50\%}$ and 20 % improvement in σ_{fail} (or 57 % improvement in specific strength) compared to those of the neat TPU. As expected, the modification of the TPU with high content of the stiff CNT filler decreased the failure strain relative to the TPU matrix and in the nanocomposite sheets the failure strain increases with the increasing TPU content for all the compositions. However, at an equivalent strain, the absorbed energy per volume of the nanocomposite is significantly higher than that of TPU (i.e. $\boldsymbol{G_{\varepsilon=20\%}}$, $\boldsymbol{G_{\varepsilon=50\%}}$ and $\boldsymbol{G_{\varepsilon=100\%}}$ in Table 2). The ultimate absorbed energy before fracture or tensile toughness ($\boldsymbol{G_t}$) was measured for all CNPU compositions. The CNPU-80 offered the highest tensile toughness as compared to all specimens (including neat TPU).

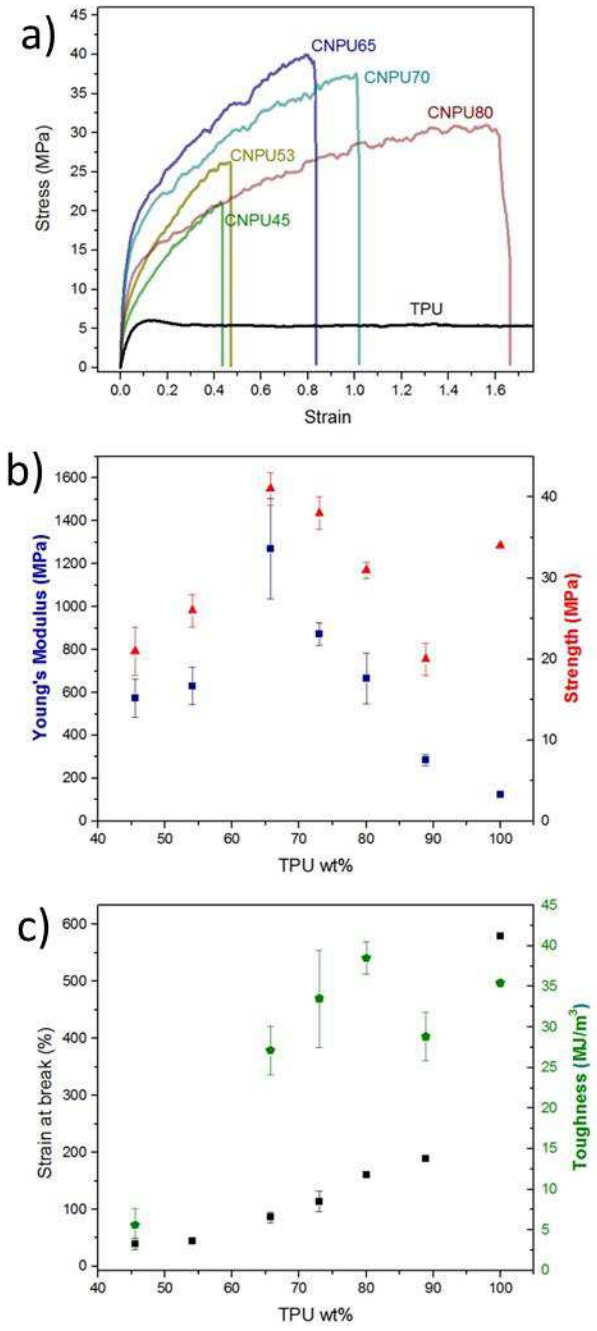

Figure 4. Typical tensile stress-strain curves for CNT-TPU sheets of different CNT/TPU wt. ratios (a) and a summary of the mechanical properties (b and c) showing the Young's Modulus (■), tensile strength (▲), strain at break (■) and toughness (●) . Samples were prepared in the acetone/methanol mixture with CNTs from Nanocyl.

Table 2. Mechanical properties of the CNT-TPU composite sheets, with comparisons to CNT buckypaper (Nanocyl MWCNTs) and the neat TPU. The CNT-TPU samples were prepared in the acetone/methanol mixture

	E	σ_{fail}	ε_{fail}	G_t	$\sigma_{\varepsilon=20\%}$	$\sigma_{\varepsilon=50\%}$	$\sigma_{\varepsilon=100\%}$	$G_{\varepsilon=20\%}$	$G_{\varepsilon=50\%}$	$G_{\varepsilon=100\%}$
	MPa	MPa	(%)	MJ/m^3	MPa	MPa	MPa	MJ/m^3	MJ/m^3	MJ/m^3
MWCNT	160±57	1±0.5	1.5±0.5							
CNPU-45	575±89	21±3	39±9.8	6±2.2	14.9±0.6	24.3±1	-	2.0±0.1	8.1±0	-
CNPU-55	630±88	26±2	44±4.4	8.0±1.4	17.9±0.8	29.1±1.5	-	2.4±0.1	9.9±0	-
CNPU-65	1270±230	41±2	86±8.6	27±2.6	26.5±2.2	34.9±3.1	-	4.1±0.3	13.4±1.2	-
CNPU-70	870±51	38±2	114±19	33±6.5	21.5±1.6	29.9±1.7	37.1±1.6	3.3±0.3	11.1±0.7	27.8±1.1
CNPU-80	670±120	31±1	160±6.1	38±2.0	16.2±0.8	22.0±1.0	27.9±0.6	2.6±0.1	8.3±0.3	21.0±0.6
CNPU-90	290±27	20±2	189±2.4	29±3.1	11.0±1.4	13.3±1.7	15.8±1.6	1.7±0.2	5.4±0.7	12.7±1.6
XL-CNPU-65[a]	2030±350	99±14	20±3.0	14±3.7	102±15	-	-	13.8±2	-	-
UAF-472	120±8	34[b]	580[b]	35[b]	5.8±0.3	5.3±0.3	5.4±0.3	1.0±0.1	2.6±0.1	5.3±0.3

[a] Prepared with XL-CNTs, XL-CNT/TPU=35:65 weight ratio (29 vol.% void), density 0.984 g/cm^3

[b]From the manufacturer data sheet. The data sheet information is used here as the neat TPU (UAF-472) did not fail within the displacement limit of the micro-tensile test frame (see Figure S2).

An additional sample was also fabricated with longer nanotubes (XL-CNPU-65 sample in Table 2 using XL-CNTs) at the optimal CNT/TPU weight ratio. It has been shown that the CNT aspect ratio plays an important role in the overall performance of nanocomposites, but longer nanotubes are generally more difficult to disperse and process. Nanocomposites incorporating XL-CNTs with a significantly higher aspect ratio were also successfully fabricated using the

one-step filtration method. The tensile properties significantly increased as compared to the shorter CNTs, although the nanotube content was approximately the same as the previous sheets (17 vol.% vs. 19 vol.%, respectively). In this case ~ 17 fold improvements in E, ~18 fold improvement in $\sigma_{\varepsilon=20\%}$ and 3 fold improvement in σ_{fail} (3.5 fold improvement in specific strength) compare to those of the neat TPU were observed. These improvements in tensile properties are comparable to current literature values that use the buckypaper infiltration or solution casting methods.[4,9,11] The nanocomposite sheets are robust, flexible and can be integrated similarly to other fiber fabrics into conventional composite manufacturing processes to fabricate hybrid composites.[22]

AFM imaging and mechanical mapping have recently been introduced to provide quantitative elastic modulus information on soft and hard segments of polymers such as polyurethane,[23] carbon black-filled nitrile butadiene rubber[24] and polypropylene.[25] However, the AFM based measurements are generally limited to the mechanical characterization of homogeneous sample, and only a handful attempts to use this more direct imaging and mapping technique to characterize samples with complex morphology distribution. Peak Force QNM mode was conducted on selected CNT-TPU nanocomposites and pure TPU in order to compare the experimental tensile tests (macroscale) with the elastic modulus at the nano/microscale. Figure 5a shows typical height images (top panel) and elastic modulus maps (bottom panel) measured on TPU and the nanocomposites. Corresponding distributions of elastic moduli are shown in Figure 5b and the specific absolute values of elastic modulus are summarized in Table S2.

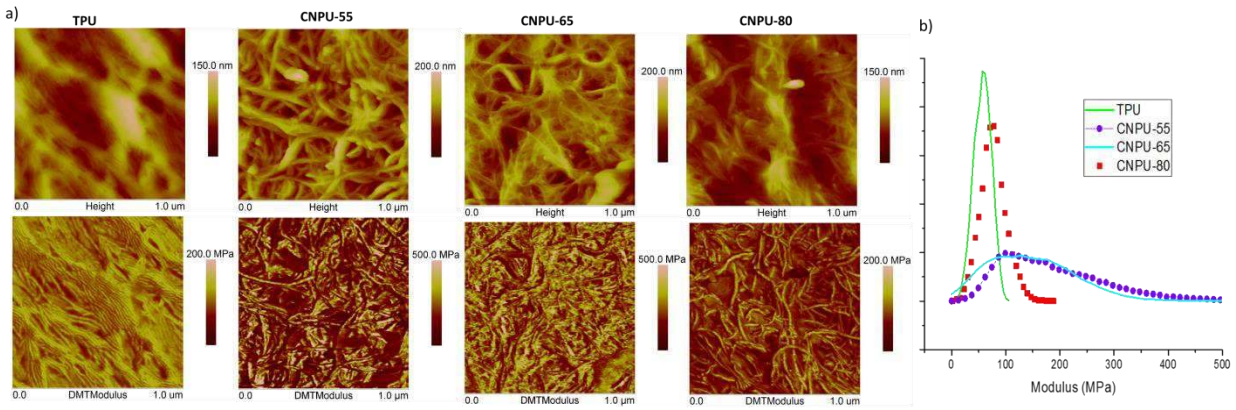

Figure 5. AFM morphology images (top panel) and elastic modulus maps (bottom panel) of TPU and CNT-TPU nanocomposites (a). Note that different vertical (z-range) scales were used to better visualize the sample morphology and elastic modulus. (b) Distributions of elastic moduli for TPU and CNT-TPU nanocomposites corresponding to images in Figure 5a

The unmodified TPU clearly shows well-separated phases in the form of ribbon-like hard domains dispersed in the soft segment phase, which can be quantified by high resolution elastic modulus mapping (Figure 5a). As shown in Figure 5b and summarized in Table S2 the distribution of modulus values for the neat TPU was narrow (compared to the nanocomposites) and centered around 60 MPa with a shoulder peak at around 30 MPa. AFM images of the CNT-TPU nanocomposites confirm the SEM surface characterization indicating the presence of voids and changes in the CNT network density as a function of composition. CNPU-55 and CNPU-65 both show high density networks of CNTs, with higher modulus than TPU but much broader distributions of elastic modulus with values ranging from a few MPa to 450 MPa, centered at 100 - 200 MPa. For CNPU-80, fewer CNTs were visualized in both the topography and modulus maps and the narrower modulus distribution (Figure 5b) resembles the neat TPU but with values centered between 90 and 140 MPa (depending on the analyzed surface areas).

Similar trends are observed from both the macroscopic, uniaxial tensile tests and the AFM mapping. Both results indicate a limit in TPU content, which determines the density of the network of CNTs and the interface contribution (fraction of the polymer phase strongly adhered to the CNTs surface), for optimal improvement in the nanocomposite stiffness. Moreover, the macroscopic values of specific modulus (Young's modulus normalized to the sample density) of CNPU-55 and CNPU-65 are very similar and both significantly higher than for CNPU-80 (1000 and 1400 MPa for CNPU-55 and CNPU-65, respectively and 600 MPa for CNPU-80) in closer agreement with the trend observed by AFM. This indicates that the elastic modulus determined by AFM measurements is probably not as influenced by the sheets porosity as tensile tests are.

To investigate the effect of a different solvent on the exfoliation of CNTs and on the properties of CNT-TPU sheets, an additional set of samples was prepared using the solvent/non-solvent approach but with DMF as the good solvent. Table S3 summarizes the composition of the CNT-TPU sheets (using Nanocyl MWCNTs) prepared from the DMF/methanol mixture. DMF is a more effective organic solvent to disperse CNTs than acetone, although the solubility of individualized CNTs is still limited to low concentrations. In this case the filtration time was usually longer than in the acetone/methanol case, despite the use of the non-solvent, which suggests that the conformation of the polymer and the interactions with the solvent are different. Table 3 summarizes the tensile properties obtained for these nanocomposite sheets at different CNT/TPU weight ratios. Samples were prepared comprising the composition range previously found to provide optimal improvement in elastic modulus and tensile strength.

Table 3. Mechanical properties of the CNT-TPU composite sheets prepared in the DMF/methanol mixture

Sample	CNT content* (vol.%)	E (MPa)	σ_{fail} (MPa)	ε_{fail} (%)	G_t (MJ/m^3)
CNPU-40-D	23	1440 ± 250	28 ± 3	36 ± 7	8 ± 2
CNPU-58-D	22	1715 ± 97	42 ± 4	50 ± 12	16 ± 5
CNPU-62-D	23	2010 ± 370	51 ± 2	61 ± 7	24 ± 4

* Prepared with CNTs from Nanocyl

For similar CNT/TPU weight ratios, higher CNT volume fractions are reached when the DMF/methanol mixture is used as compared with nanocomposites sheets obtained from the acetone/methanol mixture (23 vs. 19 vol.%). The tensile properties exhibit the same trend previously observed with increasing TPU wt.%, but with greater improvements in mechanical properties (e.g. ~17 fold improvement in elastic modulus, and 50 % improvement in tensile strength compare to those of the neat TPU) as compared to CNT-TPU sheets prepared in the acetone/methanol mixture at the optimal composition. This indicates that the use of a good TPU solvent that can also exfoliate the CNTs more efficiently leads to a better packing in the nanocomposite sheets.

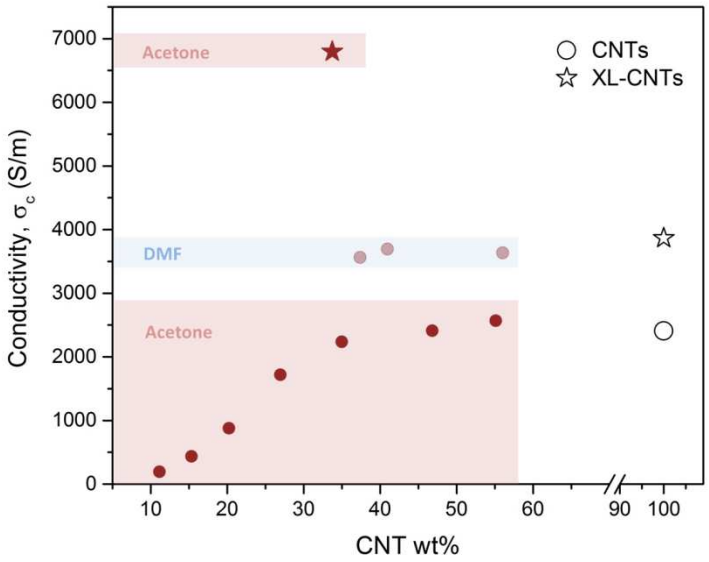

Figure 6. Electrical conductivities for CNT-TPU nanocomposite sheets (filled symbols) prepared by the solvent/non-solvent one-step filtration method using different types of CNTs and different good solvents. Electrical conductivities for CNT buckypapers without TPU (unfilled symbols) are shown for comparison.

One important aspect of lightweight nanocomposite materials is the opportunity for added functionalities while improving mechanical performance. Figure 6 shows a summary of the electrical conductivity measured for the obtained CNT-TPU composites of different compositions (i.e., CNT wt.% and CNT type) and fabricated with different solvent/non-solvent mixtures. The conductivity values here fall within the typical range reported for randomly oriented buckypaper sheets (~1,000-10,000 S/m, e.g.[26-29]). Nanocomposites prepared in the acetone/methanol mixture (using MWCNTs from Nanocyl) in the composition range between CNPU-45 to CNPU-65 (Table 1), where the CNT vol.% is almost constant, exhibit an electrical conductivity similar to the pristine buckypaper. This indicates that the number of conductive paths is not significantly decreased by the increasing addition of the insulating matrix and that during the fabrication method a similar number of nanotube-nanotube junctions are still present.

The electrical conductivity results support the description that in this composition range, even though the CNTs or CNT bundles are being increasingly covered by the TPU, further CNT exfoliation is also occurring and only a small decrease in electrical conductivity is observed. However, above ~65 wt.% TPU (bellow 35 wt.% CNTs) the electrical conductivity significantly decreases as the TPU wt.% increases in agreement with the data for TPU adsorption on the CNTs (Figure 3A), its effect on the sheets morphology and the systematic decrease in CNT vol.%. The effectiveness of the fabrication method to facilitate processing and increase CNTs exfoliation in the final sheet was also demonstrated for the case of longer CNTs. Figure 6 also includes electrical conductivity values for the nanocomposite sheet (XL-CNPU-65) prepared by the one-step filtration method in the acetone/methanol mixture and a buckypaper fabricated with XL-CNT using sodium cholate as dispersant in water. In this case, as expected the electrical conductivity of the buckypaper fabricated with the longer tubes shows an increase (almost 2 fold) over the shorter CNTs. However, in the CNT-TPU composite sheets almost 3 fold increase is observed and the conductivity is much higher than the buckypaper sample, indicating that the solvent/non-solvent approach with TPU is more effective than the sodium cholate surfactant for debundling and packing these long CNTs.

Electrical conductivity measurements for samples prepared from the DMF/Methanol solvent mixture also suggest that using a better solvent for the CNTs leads to more efficient debundling and formation of a more effective CNT network. The electrical conductivity of CNT-TPU sheets prepared using this solvent system is significantly higher compared to the pristine buckypaper and the CNT-TPU sheets prepared from the acetone/methanol mixture, which provides further indication of a better exfoliation of the CNT bundles in these nanocomposite sheets producing nanocomposite sheets with higher CNT volume fraction.

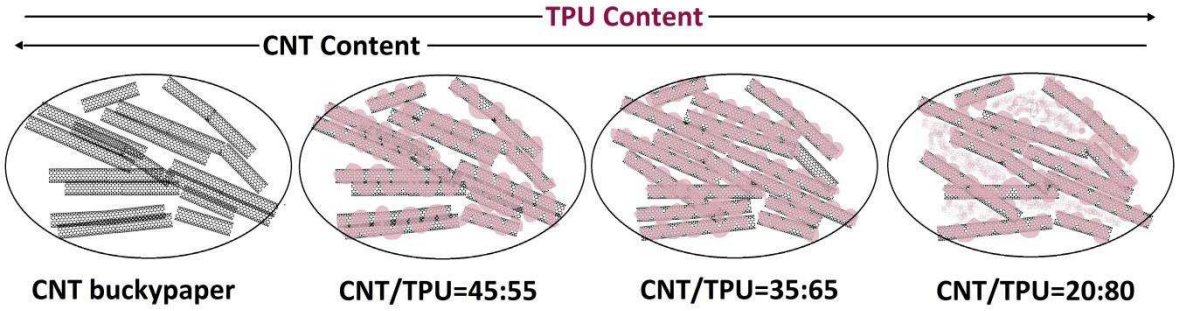

Figure 7. Schematic representation of morphological changes in the nanocomposite sheets as a function of the CNT/TPU weight ratio

Figure 7 schematically represents the morphological evolution of the CNT-TPU sheets as a function of the CNT/TPU weight ratio according with results discussed above. As the TPU wt.% increases, up to a 35:65 CNT/TPU weight ratio (i.e. sample CNPU65 in the acetone/methanol mixture), the incremental addition of TPU improves CNT exfoliation by forming a stable shell around the CNTs. In that composition range the CNT vol.% is almost constant (no significant increase in the sheet thickness), and an optimal packing is achieved with increasing CNT exfoliation. When the TPU wt.% increases above the CNT surface-coverage saturation point, free polymer coexists with the CNT-TPU fibers. The free TPU not only reduces the void vol.% but also increases the CNT-CNT inter-tube (and/or inter-bundle) distance, which decreases the CNT vol.% in the nanocomposite sheets. These morphological changes explain the observed trends in composition, tensile properties and electrical conductivity.

The one-step solvent/non-solvent processing method has proven effective for the fabrication of light-weight (0.5 to 1.1 g/cm^3), high-CNT-content nanocomposite sheets with tailored composition, and tailored mechanical and electrical properties. Even without optimal CNT

individualization, which usually requires large volumes of solvent or covalent surface modification and can make scaling-up more difficult (i.e., large solvent quantities, very long filtration times, difficulties to attaining reproducible high power sonication at larger scale), it was possible to improve the CNT exfoliation and optimize the interface interaction with the matrix.

CONCLUSION

We have developed a one-step filtration method for the fabrication of CNT-TPU composite sheets with high CNT content and precise control of the composition. Consequently, electrically conductive materials with tailorable properties (e.g. porosity, stiffness, strength and toughness) and shapes can be fabricated. The use of a solvent/non-solvent mixture to fabricate the nanocomposite sheets has proven to be effective to improve the processing conditions by significantly reducing filtration times and avoiding the need to disperse the CNTs in large volume of solvents to improve CNTs exfoliation.

Equilibrium sorption experiments were conducted to evaluate the CNT-TPU interaction and explain the morphological and processing changes occurring as a function of increasing TPU content in different solvents and in an acetone/methanol mixture. It was shown that a solvent/non-solvent mixture increases the adsorption uptake of TPU by the CNTs as compared to samples prepared in a good solvent only. In the resulting nanocomposite sheets, the TPU is observed as a coating on the CNTs. Because of the CNT-TPU fibril morphology and relatively low C_{eq} of TPU in the acetone/methanol mixture, the CNT-TPU nanocomposites can be recovered by filtration in a very short time as a sheet made of randomly oriented CNT-TPU fibers. Tensile properties and electrical conductivity show an optimum near the same

composition. As the TPU wt.% increases the tensile strength and modulus initially increase, with maximum values at the CNT/TPU composition of 35:65 by weight, and then decrease with increasing TPU content. This trend was also explained as a result of the morphological changes occurring as a function of increasing the TPU wt.%. At the 35:65 weight ratio a better CNT exfoliation and optimal CNT surface coverage is achieved (optimized CNT/TPU interface), which in turn leads to an optimal packing of CNT-TPU fibers. With further TPU addition (above 35:65 weight ratio) the deposition of free TPU occurs (cooperative adsorption), which increases the inter-tube distance and produces thicker sheets with a lower CNT vol.% (lower reinforcement), although optimal tensile toughness was achieved at the 20:80 weight ratio. The use of a better solvent to disperse the CNTs led to a higher CNT vol.% in the nanocomposite sheets, as seen for sheets fabricated from a DMF/methanol mixture. Further improvements in tensile properties and electrical conductivity were observed in this solvent mixture as compared to materials prepared from the acetone/methanol mixture. This result also supports the hypothesis that a better packing is achieved when the CNT bundles are better exfoliated at the optimal surface coverage. AFM imaging and mechanical mapping analyses confirmed the morphological characterization by SEM and were used to obtain localized modulus values at the nanoscale. In addition, simultaneously measured elastic modulus maps also directly correlated to the topography of the samples at the micro- and nanometer scales, which provided basic localized trends from different compositions and can be compared with macroscopic results.

The morphological changes explain the observed trends in composition, mechanical properties and electrical conductivity. The one-step solvent/non-solvent process has been shown to be a convenient method for the fabrication of light-weight, high CNT content nanocomposite sheets with tailored mechanical and electrical properties. The features of the process are also expected

to be favorable for scaling to larger sheets and higher production rate, which is presently under investigation along with the use of these nanocomposite fabrics as a component in laminated composites and for coatings.

ASSOCIATED CONTENT

Supporting Information. Composition of CNT-TPU sheets prepared and additional SEM images. Summary of elastic modulus calculated by AFM.

AUTHOR INFORMATION

Corresponding Author

*Yadienka.Martinez-Rubi@nrc-cnrc.gc.ca (Y. Martinez-Rubi), Benoit.Simard@nrc-cnrc.gc.ca (B. Simard)

Author Contributions

The manuscript was written through contributions of all authors. All authors have given approval to the final version of the manuscript.

ACKNOWLEDGMENT

Technical assistance from Daesun Park and Gordon Chan is gratefully acknowledged. This work was supported by NRC programs on Security Materials Technology and Advanced Manufacturing.

REFERENCES

1. Spitalsky, Z.; Tasis, D.; Papagelis K, Galiotis, C. Carbon nanotube–Polymer Composites: Chemistry, Processing, Mechanical and Electrical Properties. Progress in Polymer Science 2010, 35, 357-401.

2. Ma, P.C.; Siddiqui, N.A.; Marom, G.; Kim, J.K. Dispersion and Functionalization of Carbon Nanotubes for Polymer-Based Nanocomposites: A review. Composites A. 2010, 4,1345-1367.

3. Mittal, V. Polymer Nanotube Nanocomposites Synthesis, Properties and Applications, Scrivener Publishing: Massachusetts, 2010.

4. Fernández-d'Arlas, B.; Khan, U.; Rueda, L.; Martin, L.; Ramos, J. A.; Coleman, J. N.; González, M. L.; Valea, A.; Mondragon, I.; Corcuera, M. A.; Eceiza, A. Study of the Mechanical, Electrical and Morphological Properties of PU/MWCNT Composites Obtained by two Different Processing Routes. Compos. Sci. Technol.2012, 72, 235–242.

5. Wang, Z.; Liang, Z.; Wang, B.; Zhang, C.; Kramer, L. Processing and Property Investigation of Single-Walled Carbon Nanotube (SWNT) Buckypaper/Epoxy Resin Matrix Nanocomposites. Compos. A 2004, 35, 1225-1232.

6. Cheng, Q.; Wang, B.; Zhang, C.; Liang, Z. Functionalized Carbon-Nanotube Sheet/Bismaleimide Nanocomposites: Mechanical and Electrical Performance Beyond Carbon-Fiber Composites. Small 2010, 6, 763–767.

7. Cano, R.J.; Grimsley, B.W.; Czabaj, M.W.; Hull, B. T.; Siochi, E. J. Processing and Characterization of Carbon Nanotube Composites. SAMPE Seattle 2014 International Conference and Exhibition, Soc. for the Advancement of Material and Process Engineering 2014.

8. Miller, S.G.; Williams,T.S.; Baker, J.S., Solá, F.; Lebron-Colon, M.; McCorkle, L.S.; Wilmoth, N.G.; Gaier, J.; Chen, M.; Meador, M.A. Increased Tensile Strength of Carbon Nanotube Yarns and Sheets through Chemical Modification and Electron Beam Irradiation. ACS Appl. Mater. Interfaces 2014, 6, 6120–6126.

9. Han, J.-H.; Zhang, H.; Chen, M.-J.; Wang, G.-R.; Zhang, Z. CNT Buckypaper/Thermoplastic Polyurethane Composites with Enhanced Stiffness, Strength and Toughness, Compos. Sci. Technol. 2014, 103, 63–71.

10. Koerner, H.; Liua, W.; Alexander, M.; Mirau, P.; Dowty, H.; Vaia, R. A. Deformation–morphology correlations in electrically conductive carbon nanotube—thermoplastic polyurethane nanocomposites. Polymer, 2005, 46, 4405–4420

11. Blighe, F. M.; Blau, W. J.; Coleman, J. N. Towards Tough, yet Stiff, Composites by Filling an Elastomer with Single-Walled Nanotubes at very High Loading Levels", Nanotechnology 2008, 19 415709- 415715.

12. Van der Pauw, L.J. A Method for Measuring Specific Resistivity and Hall Effect of Discs of Arbitrary Shape. Phillips Research Reports 1958, 13, 1.

13. Gojzewski, H.; Imre, B.; Check,C.; Chartoff, R.; Vancso, J. Mechanical Mapping and Morphology Across the Length Scales Unveil Structure-Property Relationships in

Polycaprolactone Based Polyurethanes. J. Polym. Sci., Part B: Polym. Phys. 2016, 54, 2298–2310.

14. Wang, J.-N.; Zhang, Y.-L.; Liu, Y.; Zheng, W.; Lee, L. P.; Sun, H.-B. Recent Developments in Superhydrophobic Graphene and Graphene-Related Materials: from Preparation to Potential Applications, Nanoscale 2015, 7, 7101–7114.

15. Silva, G. G.; Rodrigues, M. T. F.; Fantini, C.; Borges, R. S.; Pimenta, M. A.; Carey, B. J.; Ci, L.; Ajayan, P. M. Thermoplastic Polyurethane Nanocomposites Produced via Impregnation of Long Carbon Nanotube Forests. Macromol. Mater. Eng. 2011, 296, 53–58

16. Che, J.; Chen, P.; Chan-Park, M. B. High-Strength Carbon Nanotube Buckypaper Composites as Applied to Free-Standing Electrodes for Supercapacitors. J. Mater. Chem. A, 2013, 1, 4057.

17. Treybal, R.E. Mass-Transfer Operations, McGraw-Hill: New York, 1981.

18. Akl, M. A.; Abou-Elanwar, A. M. Adsorption Studies of Cd (II) from Water by Acid Modified Multiwalled Carbon Nanotubes. J Nanomed Nanotechnol 2015, 6, 327. doi:10.4172/2157-7439.1000327.

19. Peter, K. T.; Vargo, J.D.; Rupasinghe, T. P.; De Jesus, A.; Tivanski, A. V.; Sander, E. A.; Myung, N. V. Cwiertny, D. M. Synthesis, Optimization, and Performance Demonstration of Electrospun Carbon Nanofiber−Carbon Nanotube Composite Sorbents for Point-of-Use Water Treatment. ACS Appl. Mater. Interfaces 2016, 8, 11431−11440.

20. Juang, R.-S.; Wu, F.-C; and Tseng, R.-L. Adsorption Isotherms of Phenolic Compounds from Aqueous Solutions onto Activated Carbon Fibers. J. Chem. Eng. Data 1996, 41, 487-492.

21. Martinez Rubi, Y.; Retuert, J.; Yazdani-Pedram, M.; Colfen, H. Transparent Semiconductor–Polymer Hybrid Films with Tunable Optical Properties. J. Mater. Chem., 2007, 17, 1094–1101.

22. Martinez-Rubi, Y.; Ashrafi, B.; Jakubinek, M.; Denommee, S.; Guan, J.W.; Simard. B. Integration of Nanotube Paper into UHMWPE Multilayer Structures: Towards Increased Impact Resistance", Proceedings 10th Canada-Japan Workshop on Composites, Canada, 2014.

23. Schön, P.; Bagdi, K.; Molnar, K.; Markus, P.; Pukanszky, B.; Vancso, G. J. Quantitative Mapping of Elastic Moduli at the Nanoscale in Phase Separated Polyurethanes by AFM. Eur. Polym. J. 2011, 47, 692–698, 2011.

24. Qu, M.; Deng, F.; Kalkhoran, S. M.; Gouldstone, A.; Robisson, A.; Van Vliet, K. J. Nanoscale Visualization and Multiscale Mechanical Implications of Bound Rubber Interphases in Rubber-Carbon Black Nanocomposites Soft Matter 2011, 7, 1066–1077.

25. Liparoti, S.; Sorrentino, A.; Speranza,V. Micromechanical Characterization of Complex Polypropylene Morphologies by HarmoniX AFM. Int. J. Polym. Sci. 2017, 2017, ID 9037127, 12 pages.

26. Zhang, J.; Jiang, D.; Peng, H.-X.; Qin, F. Enhanced Mechanical and Electrical Properties of Carbon Nanotube Buckypaper by in situ Cross Linking. Carbon 2013, 63, 125.

27. Jakubinek, M.B.; Ashrafi, B.; Guan, J.; Johnson, M.B.; White, M.A.; Simard. B. 3D Chemically Cross-linked Single-Walled Carbon Nanotube Buckypapers. RSC Advances 2014, 4, 57564.

28. Wang, D.; Song, P.; Liu, C.; Wu, W.; Fan. S. Highly Oriented Carbon Nanotube Papers Made of Aligned Carbon Nanotubes. Nanotechnology 2008, 19, 075609.27.

29. Sakurai, S.; Kamada, F.; Futaba, D.N.; Yumura, M.; Hata, K. Influence of Lengths of Millimeter-Scale Single-Walled Carbon Nanotube on Electrical and Mechanical Properties of Buckypaper. Nanoscale Res. Lett. 2013, 8, 546.

TOC